Research Article | Vol. 26, No. 9 | 30 Apr 2018 | OPTICS EXPRESS 11737
Optics EXPRESS

Selective coupling of Whispering Gallery Modes in film coated micro-resonators

ANDREA BARUCCI,[1] IMMACOLATA ANGELICA GRIMALDI,[2] GIANLUCA PERSICHETTI,[2] SIMONE BERNESCHI,[1,*] SILVIA SORIA,[1] BRUNO TIRIBILLI,[3] ROMEO BERNINI,[2] FRANCESCO BALDINI,[1] AND GUALTIERO NUNZI CONTI[1,4]

[1]*IFAC-CNR, Institute of Applied Physics "N. Carrara", Via Madonna del Piano 10, 50019 Sesto Fiorentino (FI), Italy*
[2]*IREA-CNR, Institute for Electromagnetic Sensing of the Environment, Via Diocleziano 328, 80124 Napoli, Italy*
[3]*ISC-CNR, Institute of Complex Systems, Via Madonna del Piano 10, 50019 Sesto Fiorentino (FI), Italy*
[4]*Centro Fermi - Museo Storico della Fisica e Centro Studi e Ricerche "Enrico Fermi", Compendio del Viminale, Piazza del Viminale 1, 00184 Roma, Italy*
**s.berneschi@ifac.cnr.it*

Abstract: Whispering Gallery Mode (WGM) micro-resonators like microspheres or microtoroids are typically used as high-Q cavity substrate on which a functional film coating is deposited. In order to exploit the coating properties a critical step is the efficient excitation of WGMs mainly contained inside the deposited layer. We developed a simple method able to assess whether or not these modes are selectively excited. The method is based on monitoring the thermal shift of the excited resonance, which uniquely depends on the thermo-optic coefficient and on the thermal expansion coefficient of the material in which the mode is embedded.

OCIS codes: (140.4780) Optical resonators; (140.3945) Microcavities; (310.0310) Thin films; (130.5460) Polymer waveguides.

References and links

1. G. C. Righini, S. Berneschi, G. Nunzi Conti, S. Pelli, E. Moser, R. Retoux, P. Féron, R. R. Gonçalves, G. Speranza, Y. Jestin, M. Ferrari, A. Chiasera, A. Chiappini, and C. Armellini, "Er3+-doped silica-hafnia films for optical waveguides and spherical resonators," J. Non-Cryst. Solids **355**(37-42), 1853–1860 (2009).
2. H. Choi and A. Armani, "High Efficiency Raman Lasers Based on Zr-Doped Silica Hybrid Microcavities," ACS Photonics **3**(12), 2383–2388 (2016).
3. B. B. Li, Y. F. Xiao, M. Y. Yan, W. R. Clements, and Q. Gong, "Low-threshold Raman laser from an on-chip, high-Q, polymer-coated microcavity," Opt. Lett. **38**(11), 1802–1804 (2013).
4. D. Ristic, A. Chiappini, M. Mazzola, D. Farnesi, G. Nunzi Conti, G. C. Righini, P. Feron, G. Cibiel, M. Ferrari, and M. Ivanda, "Whispering gallery mode profiles in a coated microsphere," Eur. Phys. J. Spec. Top. **223**(10), 1–11 (2014).
5. Y. Yin, Y. Niu, L. Dai, and M. Ding, "Polarization characteristics of gold-coated microdisk resonators," AIP Adv. **7**(9), 095008 (2017).
6. G. Palma, M. C. Falconi, F. Starecki, V. Nazabal, J. Ari, L. Bodiou, J. Charrier, Y. Dumeige, E. Baudet, and F. Prudenzano, "Design of Praseodymium-Doped Chalcogenide Micro-Disk Emitting at 4.7 μm," Opt. Express **25**(6), 7014–7030 (2017).
7. J. Riemensberger, K. Hartinger, T. Herr, V. Brasch, R. Holzwarth, and T. J. Kippenberg, "Dispersion engineering of thick high-Q silicon nitride ring-resonators via atomic layer deposition," Opt. Express **20**(25), 27661–27669 (2012).
8. A. Chiasera, Y. Dumeige, P. Féron, M. Ferrari, Y. Jestin, G. Nunzi Conti, S. Pelli, S. Soria, and G. C. Righini, "Spherical Whispering-Gallery-Mode Microresonators," Laser Photonics Rev. **4**(3), 457–482 (2010).
9. K. Gardner, Y. Zhi, L. Tan, S. Lane, Y.-F. Xiao, and A. Meldrum, "Whispering gallery mode structure in polymer-coated lasing microspheres," J. Opt. Soc. Am. B **34**(10), 2140–2146 (2017).
10. J. L. Dominguez-Juarez, G. Kozyreff, and J. Martorell, "Whispering gallery microresonators for second harmonic light generation from a low number of small molecules," Nat. Commun. **2**, 254 (2011).
11. A. K. Mallik, D. Liu, V. Kavungal, Q. Wu, G. Farrell, and Y. Semenova, "Agarose coated spherical micro resonator for humidity measurements," Opt. Express **24**(19), 21216–21227 (2016).
12. B.-B. Li, Q.-Y. Wang, Y.-F. Xiao, X.-F. Jiang, Y. Li, L. Xiao, and Q. Gong, "On chip, high-sensitivity thermal sensor based on high-Q polydimethylsiloxane-coated microresonator," Appl. Phys. Lett. **96**(25), 251109 (2010).

#321024 https://doi.org/10.1364/OE.26.011737
Journal © 2018 Received 30 Jan 2018; revised 12 Mar 2018; accepted 12 Mar 2018; published 23 Apr 2018

Optics EXPRESS

13. T. Ioppolo, V. Ötügen, and U. Ayaz, "Development of Whispering Gallery Mode polymeric micro-optical electric field sensors," J. Vis. Exp. **71**(71), e50199 (2013).
14. M. Charlebois, A. Paquet, L. S. Verret, K. Boissinot, M. Boissinot, M. G. Bergeron, and C. N. Allen, "Toward Automatic Label-Free Whispering Gallery Modes Biodetection with a Quantum Dot-Coated Microsphere Population," Nanoscale Res. Lett. **5**(3), 524–532 (2010).
15. D. Ristić, A. Rasoloniaina, A. Chiappini, P. Féron, S. Pelli, G. N. Conti, M. Ivanda, G. C. Righini, G. Cibiel, and M. Ferrari, "About the role of phase matching between a coated microsphere and a tapered fiber: experimental study," Opt. Express **21**(18), 20954–20963 (2013).
16. M. J. Humphrey, E. Dale, A. T. Rosenberger, and D. K. Bandy, "Calculation of optimal fiber radius and whispering-gallery mode spectra for a fiber-coupled microsphere," Opt. Commun. **271**(1), 124–131 (2007).
17. I. A. Grimaldi, S. Berneschi, G. Testa, F. Baldini, G. Nunzi Conti, and R. Bernini, "Polymer based planar coupling of self-assembled bottle microresonators," Appl. Phys. Lett. **105**(23), 231114 (2014).
18. K.-C. Fan, W. Wang, and H.-S. Chiou, "Fabrication optimization of a micro-spherical fiber probe with the Taguchi method," J. Micromech. Microeng. **18**(1), 015011 (2008).
19. W. Pfleging, M. Przybylski, and H. J. Brückner, "Excimer laser material processing – state of the art and new approaches in microsystem technology," Proc. SPIE **6107**, 61070G (2006).
20. V. Pini, B. Tiribilli, C. M. C. Gambi, and M. Vassalli, "Dynamical characterization of vibrating AFM cantilever forced by photothermal excitation," Phys. Rev. B **81**(5), 054302 (2010).
21. A. Barucci, S. Berneschi, A. Giannetti, F. Baldini, A. Cosci, S. Pelli, D. Farnesi, G. C. Righini, S. Soria, and G. Nunzi Conti, "Optical Microbubble Resonators with High Refractive Index Inner Coating for Bio-Sensing Applications: An Analytical Approach," Sensors (Basel) **16**(12), 1992 (2016).
22. P. Rabiei, W. H. Steier, C. Zhang, and L. R. Dalton, "Polymer Micro-Ring Filters and Modulators," J. Lightwave Technol. **20**(11), 1968–1975 (2002).
23. Y. Yang Yu, X. Qiang Sun, L. Ting Ji, G. Bing He, X. Bin Wang, Y. Ji Yi, C. Ming Chen, F. Wang, and D. Ming Zhang, "The 650-nm variable optical attenuator based on polymer/silica hybrid waveguide," Chin. Phys. B **25**, 054101 (2016).

1. Introduction

Coating of high-Q Whispering Gallery Mode (WGM) micro-resonators is generally performed in order to add the functionalities of the coating material to the unique properties of this type of resonators. A variety of fabrication techniques allows depositing film with different types of material (glass, polymers, semi-conductors, etc.) [1–7]. Silica microtoroids [2] or microspheres [3] are typically used as 'micro-resonator substrate' because they can be relatively easily fabricated and coated, and they exhibit high-Q factor and high finesse [8].

In particular, due to their high versatility and their interesting thermal, optical and mechanical properties, polymers are gaining an ever growing interest as material for WGM micro-resonators coating in a wide range of applications ranging from lasing [3,9] to nonlinear optics [10] up to sensing [11–14].

A modeling step allows determining the WGMs distribution and their overlap with the deposited layer. Typically the film thickness can be chosen in order to have just the fundamental mode mainly confined in the coating layer [15].

Finally it is necessary to implement an efficient coupling to the fundamental mode or 'layer mode' of the resonator, which is required to effectively exploit the coating properties. Generally, suitable evanescent fields overlap and right phase matching conditions between the WGMs and the propagating mode of the excitation system are required in order to achieve an efficient and selective coupling [15].

In this work we show that, by properly selecting the coupling system (either a fiber taper or an integrated waveguide) in order to fulfill phase matching conditions [16,17], we can excite either the fundamental WGM, which is mainly confined in the coating, or higher order modes, primarily confined in the silica 'bulk substrate'. For this purpose we developed a simple *ex post* method able to assess which mode is actually coupled. The method is based on monitoring the thermal shift of the excited resonance, which uniquely depends on the thermo-optic coefficient and on the thermal expansion coefficient of the material in which the mode is embedded, as in the case of temperature sensing [12]. We applied this technique to the case of an SU-8 layer deposited on a silica microsphere and main tests were performed around 770 nm wavelength, having in mind potential application in biochemical sensing and low light

Optics EXPRESS

absorption in aqueous environment. Further validation of the approach is obtained with additional considerations on the free spectral range (FSR) of the excited resonances.

2. Experiment

Microspheres were fabricated upon heating the cleaved tip of a standard SM fiber with the arc discharge of a fusion splicer. The glass partially melts and reflows to form a spherical shape under the influence of surface tension [18]. Typical spheres used in our experiment have diameters around 230 μm and pristine Q factors in excess of 10^7.

A coating of pure SU-8 2002 (Microchem Corp.) was deposited onto the microspheres through one (type 1 coated microsphere) or two dip-coating steps (type 2 coated microsphere) with a rate of 0.6 mm/sec. After each step the microsphere was soft baked at 100 °C for 10 min. The coating was photo-polymerized by an UV lamp for 20 s and, as last step, the microsphere was post baked at 100 °C for 30 min.

The thickness of the layer was measured with an atomic force microscope (AFM) after removing it in a small portion by UV excimer laser ablation through an amplitude mask [19]. The mask opening size, adopted for our purpose, was around 45 μm × 15 μm. UV irradiations were performed by means of a Lambda Physik Compex 110 KrF excimer laser source with emission at λ = 248 nm. The adopted pulse fluency was 0.037 J/cm^2 (close to the ablation threshold of around 0.04 J/cm^2 for the SU-8 bulk material [19]) and the pulses number 20.000, for a cumulative dose of 0.74 kJ/cm^2. The repetition rate was set at 10 Hz. Atomic force microscope measurements were performed by using an instrument developed in-house, based on a XYZ piezo scanner (PI-527.3CL, Physik Instrumente) and a R9 controller (RHK Technology) operating in contact mode [20]. We used a contact cantilever (CSG01- from NT-MDT Moscow, Russia) with scan speed below 20 μm/s. Scanning areas of different size, from 50 to 10 μm were selected to identify the UV exposed area and to zoom on its edges.

Polymer ridge waveguides were made by spin coating SU-8 2000.5 ($n_{SU-8} = 1.5861$) on a PMMA substrates ($n_{PMMA} = 1.4973$) followed by a direct writing photolithography process [17]. The substrates were first cleaned with isopropyl alcohol (IPA) and dried on hot plate at 70°C for 30 minutes. SU-8 was spin-coated at 1000 rpm for 30 s to achieve 0.7 μm thick layer. A pre-bake process at 70°C for 10 min. was followed by a laser direct writing photolithography (Heidelberg GmbH) at 365 nm with a power of 11.2 mW. A soft post-baking process at 70°C for 15 min. was used for crosslinking the resist. An array of channel waveguides with sizes of 2.3 μm (width) × 0.7 μm (thickness) × 7 mm (length) were fabricated.

Fiber tapers were fabricated by heating and at the same time slowly pulling a section of a SM600 fiber to form a narrow waist. A home-made cylindrical microfurnace is used for this purpose. The taper has a biconical shape with minimum waist as small as a micrometer in diameter and overall losses below 1 dB.

A tunable fiber pigtailed external-cavity laser operating between 765 nm and 781 nm, and with a linewidth of a few hundred kHz (New Focus velocity laser 6312) was used as light source to selectively excite the resonances. The laser can be finely swept at low frequency (< 1KHz) within about 120 pm and with subpicometer resolution. A fiber polarization controller is inserted before butt coupling the SM600 fiber to a polymer waveguide or splicing it to the fiber taper. After coupling with the resonator the output light is monitored using an amplified InGaAs photodiode detector (Thorlabs PDA400) connected to an oscilloscope.

We also used an unseeded fiber coupled semiconductor optical amplifier (Superlum SOA-332) as broadband source (50 nm bandwidth around 785 nm) in order to simultaneously excite more resonances within several free spectral ranges. The output spectra from the resonator is sent to an optical spectrum analyzer (Ando AQ6317B) with a wavelength resolution of 15 pm. This interrogation system was used to monitor the thermally induced shift of the resonances and to assess the free spectral range. The thermostatic cell used to

Optics EXPRESS

change the resonator temperature was similar to that described in [8] and it is sketched in Fig. 1(a) for the case of waveguide coupling.

3. Thermal shift analysis

A simple equation can be used to approximately relate an integer number l (azimuthal number) of wavelengths at resonance to the optical length of the microsphere of overall radius R ($R = R_{sil} + \delta R_{SU8}$) where $\delta R_{SU8} << R$ is the SU-8 layer thickness:

$$l\lambda = 2\pi nR \;\; 2\pi\left(\eta_{sil} n_{sil} + \eta_{SU8} n_{SU8}\right) R = 2\pi n_{eff} R \tag{1}$$

where n_{sil} (1.4539 at 770 nm) and n_{SU-8} (1.5861 at 770 nm) are the refractive indices of the silica and of the SU-8 layer, respectively, n_{eff} is the WGM effective index, and n_{sil} and η_{SU-8} are the WGM power fraction in the silica and in the SU-8 layer, respectively. The field distribution, from which these fractions are calculated can be obtained with a modeling procedure similar to that developed in [21]. By differentiating versus temperature Eq. (1) we obtain:

$$\frac{\partial\lambda}{\lambda} = \left\{\left[\frac{1}{n_{eff}}\left(\eta_{sil}\frac{n_{sil}}{T} + \eta_{SU8}\frac{\partial n_{SU8}}{\partial T}\right)\right] + \frac{1}{R}\left[\left(\frac{1}{R_{sil}}\frac{\partial R_{sil}}{\partial T}\right)R_{sil} + \left(\frac{1}{\delta R_{SU8}}\frac{\partial \delta R_{SU8}}{\partial T}\right)\delta R_{SU8}\right]\right\}\partial T \tag{2}$$

where $\partial n_{sil}/\partial T$ (1.28 x 10^{-5} K^{-1}) and $\partial n_{SU-8}/\partial T$ (values in the range −1.1 x 10^{-4} K^{-1} at 1550 nm [22] to −1.8 x 10^{-4} K^{-1} at 650 nm [23]) are the thermo-optic coefficients of silica and SU-8, respectively, $1/R_{sil}\partial R_{sil}/\partial T$ (5.5 x 10^{-7} K^{-1}) and $1/R_{SU-8}\partial R_{SU-8}/\partial T$ (5.2 x 10^{-5} K^{-1}) are the thermal expansion coefficients of silica and SU-8, respectively.

Calculations show that the terms taking into account the thermo-optic coefficients are much larger than those related to thermal expansion. In fact, for WGMs mainly contained in the SU-8 layer the thermo-optical induced blue shift around 770 nm is between 53 and 86 pm/K while for those in the silica the shift towards the red is of the order of 7 pm. On the contrary the maximum shift due to thermal expansion effects is below few 10^{-6}/K (i.e. below 2 pm/K for layers 4 μm thick or thinner) for microsphere radii of the order or in excess of 100 μm and, in the cases under investigation, it can be neglected. We therefore expect to observe a significant blue shift for the WGMs that are mainly in the polymer, then decreasing shift values when the WGM starts to enter the silica, down to a small red shift (at least in principle) for those entirely contained in the bulk silica microsphere substrate.

4. Results and discussion

In order to assess the layer thickness, AFM data processing was performed on the topographic images with the free software Gwyddion 2.49, an SPM data visualization and analysis tool (http://gwyddion.net). Fig. 1(b) shows the profile of the SU-8 coating measured crossing the region where the polymer was removed by UV ablation. A 32 x 10 μm^2 3D scan is shown in the inset. The thicker layer deposited with two dip-coating steps was measured to be 650 ± 30 nm, and we assumed the thickness of the layer deposited with a single step to be half of it.

Optics EXPRESS

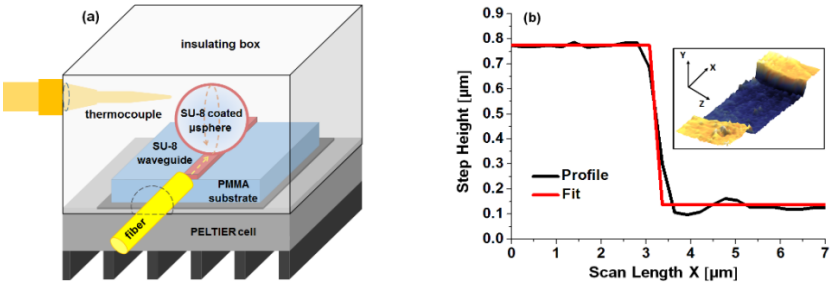

Fig. 1. (a) Sketch of the experimental set-up adopted for WGMs thermal tuning schematizing the Peltier cell and the thermocouple. (b) AFM profile of the SU-8 layer thickness deposited on the silica microsphere surface with two dip-coating processes. The inset shows a 3D plot of a surface portion after UV laser ablation of the SU-8 coating.

We demonstrate efficient coupling to the thicker SU-8 layer deposited on the silica microsphere by using an SU-8 waveguide as coupler. The calculated effective refractive indices at 770 nm for the TE and TM modes are $n_{TE} = 1.5356$, and $n_{TM} = 1.5298$, respectively. The waveguide is kept in contact with the resonator assuring improved system robustness for practical applications. Figure 2(a) presents two sets of the same resonances excited at two different temperatures (25.8 °C and 27.8 °C) by using the SOA based ultra-broadband source.

The actual blue shift due to thermal effect that we measured on the waveguide coupled resonances was of 138 ± 13 pm for about 2 K (69 pm/K) of temperature increase (around room temperature), as shown in Fig. 2(a). This result is compatible with the mode being effectively confined in the SU-8 layer, or in other words, is the demonstration of efficient coupling to WGMs mainly confined in the polymer. In fact, as shown in Fig. 3(a), the numerical calculations show that the first WGM (fundamental mode) is mainly (90%) confined in the polymer for the thicker (type 2) layer.

On the contrary, as shown in Fig. 2(b), when a silica fiber taper is used as coupler the resonances show minimal blue shift (about 3.3 pm/K) under thermal heating, indicating that the excited WGMs are mainly confined in the bulk silica. Calculations in Fig. 3(a) confirm that below 0.7 μm also the second WGM is mainly in the silica substrate. Typical resonances observed by fine scanning around 770 nm exhibit Q factors up to $5x10^5$ (see inset of Fig. 2(b)). The coupling can be explained because, when using a taper, tunneling of the polymer layer is possible by (mode and) phase matching higher order WGMs, as it can be inferred in Fig. 3(b).

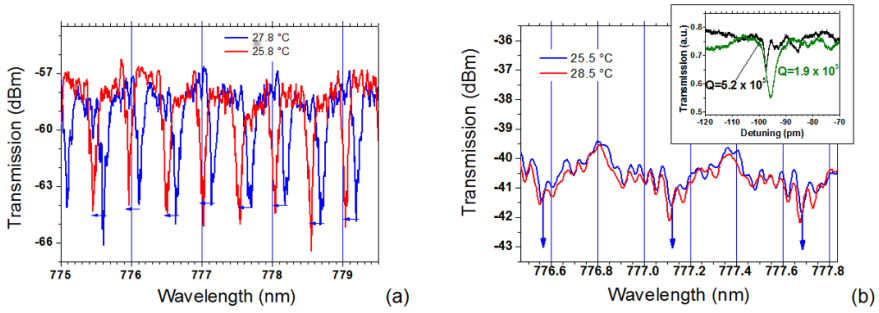

Fig. 2. (a) Resonance spectra showing blue shift of *waveguide coupled* coated microsphere (type 2, thicker coating) under thermal heating of the cavity. Average shift is 138 pm for about 2°C. Measured average FSR is 512 pm.(b) Resonance spectra showing minimal shift of *taper-coupled* coated microsphere (type 2) under thermal heating of the cavity. Average shift is below 10 pm for about 3°C. Measured average FSR is 565 pm. (inset) Typical resonances observed after fine scanning around 770 nm, showing Q factors up to $5x10^5$.

Optics EXPRESS

Indeed, Fig. 3(b) presents the dispersion curves at 770 nm for the effective refractive indices of the first four radial WGMs (TE and TM) as a function of the SU-8 thickness of a coated silica microsphere of 234 μm in diameter. The pink vertical regions represent the measured polymer thickness ranges for the layers deposited on the silica microsphere with a single or two dip-coating steps, respectively. The light blue horizontal region corresponds to the effective index range of the fundamental mode of the biconical fiber tapers we used [15], and the overlap with higher order radial modes within the tested layer thicknesses can be clearly observed. The light blue horizontal lines represent the effective indices for the TE (solid line) and the TM (dashed line) waveguide modes. TE mode crosses the fundamental WGM dispersion curve in the type 2 microsphere coating thickness range, thus fulfilling the phase matching conditions. No coupling was instead obtained from the waveguide to the microsphere with the thinner layer. The reason is that the waveguide effective index is too high compared with the fundamental WGM index of the type 1 microsphere, as shown in Fig. 3(b). On the contrary coupling from the fiber taper to higher order modes was easily accomplished, similarly to the case of the thicker layer presented above. All the simulations where performed in air but similar results were found considering water as external medium.

To further validate these results we analyzed the FSR values for the mode coupled either with the waveguide or with the taper. Indeed from Eq. (1) the FSR in wavelength for $\Delta l = 1$ can be written as [15]:

$$\Delta\lambda_{\Delta l=1} = \frac{\lambda^2}{c}\Delta\nu_{\Delta l=1} = \frac{\lambda^2}{2\pi\left(\eta_{sil}n_{sil} + \eta_{SU8}n_{SU8}\right)R}. \tag{4}$$

We observe from Fig. 2(a) that the measured FSR is 512 ± 15 pm, which is about the value obtained from Eq. (4) for a WGM entirely in the SU-8 layer ($\eta_{SU-8} \approx 1$), giving an additional demonstration that the modes excited by the waveguide are in the polymer layer. Analogously, (see Fig. 2(b)), the modes excited by the taper are separated by 565 ± 5 pm, which is about the value obtained from Eq. (4) for a WGM mainly confined in the silica substrate ($\eta_{sil} \approx 1$).

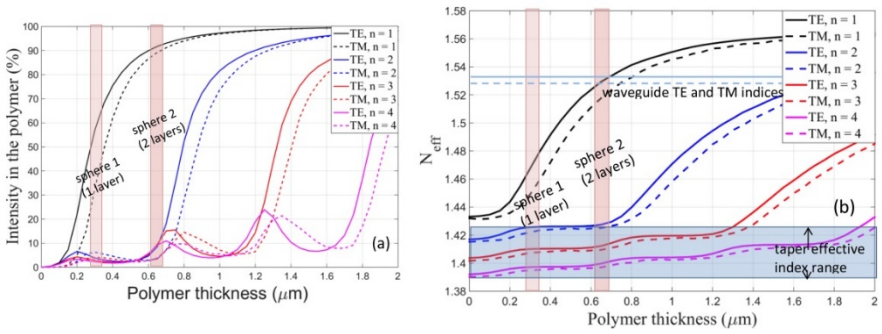

Fig. 3. (a) WGM power percentage inside the SU-8 film vs film thickness calculated at 770 nm for the first four radial WGMs (TE and TM polarization) in a coated silica microsphere of 234 μm in diameter surrounded by air. The two pink vertical regions represent the measured polymer thickness ranges for the layers deposited on the microsphere with a single or two dip-coating steps, respectively. (b) Dispersion curves showing the effective refractive indices of the same four modes vs the polymer thickness. Horizontal light blue lines show the coupling polymer waveguide effective refractive indices for the TE and TM modes. The light blue horizontal region corresponds to the effective index range of the biconical fiber tapers (with diameters between 1 μm and 2 μm).

5. Conclusions

In this work we developed a simple method able to assess which WGM is actually coupled in coated microsphere resonators. We show that, depending on the coupling system (either an

Optics EXPRESS

integrated waveguide or a fiber taper) different phase matching conditions are fulfilled, so that we can excite either the fundamental WGM, which is mainly confined in the coating, or higher order modes, primarily confined in the silica sphere 'substrate'. The demonstration is based on monitoring the thermal shift of the resonances excited in a polymer coated silica microsphere. Typically, the shift uniquely depends on the thermo-optic coefficient of the material in which the mode is embedded and therefore we can easily assess if the WGM is mainly in the polymer or in the silica (unless the coefficients are the same). A further proof of the validity of the approach is obtained considering the FSR of the excited modes which depends on the refractive index of the material in which the mode is confined.

Funding

This research study was partially supported by Ente Cassa di Risparmio di Firenze (project No. 2014.0770A2202.8861), Centro Fermi (project "MiFo"), European Community (HEMOSPEC project FP7 – 611682) and I-AMICA project (PONa3_00363).

Acknowledgments

We thank Mr. Franco Cosi from IFAC-CNR for manufacturing the tapers.